Emittance Growth during Bunch Compression in the CTF-II

H. Braun, F. Chautard, R. Corsini, T. O. Raubenheimer,* and P. Tenenbaum*
PS Division, CERN, Geneva, Switzerland
(Received 30 March 1998)

Measurements of the beam emittance during bunch compression in the CLIC Test Facility (CTF-II) are described. The measurements were made with different beam charges and different energy correlations versus the bunch compressor settings which were varied from no compression through the point of full compression and to overcompression. Significant increases in the beam emittance were observed with the maximum emittance occurring near the point of full (maximal) compression. Finally, evaluation of possible emittance dilution mechanisms indicates that coherent synchrotron radiation was the most likely cause.

PACS numbers: 29.27.Bd, 41.60.Ap, 41.75.Lx

Magnetic bunch compressors have been and will be utilized in many high-energy electron accelerators to increase the longitudinal density of a particle beam. In particular, they are important in linear colliders, where short bunches are needed because of the short depth of focus at the interaction point, and in short wavelength FELs, where high peak current is needed to reduce the optical gain length.

The compressors operate by first creating an energy variation along the length of the bunch and then passing the bunch through a series of bending magnets in which the path length is energy dependent. By appropriately choosing the energy correlation and magnet strengths, the bunch can be compressed as desired and, because the forces involved are conservative, the longitudinal and transverse phase-space densities should be conserved.

The conservation of the transverse phase-space density, referred to as the transverse beam emittance, is usually of extreme importance—this is especially true in linear colliders and short wavelength FELs whose performance is very sensitive to the transverse emittances. There are a number of sources of emittance dilution which can increase the emittances, decreasing the phase-space density. The most obvious are chromatic effects that are important because of the large energy spread (typically a few percent) that is needed to compress the bunch length; thus the compressor optics are usually achromatic to second or higher order. Other standard sources of dilution include the longitudinal wakefields and the "classical" longitudinal space charge force which is inversely proportional to the square of the beam energy $1/\gamma^2$; these break the achromaticity of the optics by generating small energy changes within the compressor.

Recently, as designs have started requiring shorter bunches and smaller emittances, the more subtle issue of what happens as the beam is deflected in the bending magnets has been discussed. This includes the transformation of the longitudinal space charge force in the curved geometry [1] as well as the coherent synchrotron radiation [2–6]. The resulting emittance dilution, which is independent of the beam energy, appears to place very stringent limits on many of the future bunch compressor designs. Coherent synchrotron radiation itself has been observed in special experiments [7,8], but, at this time, the effect on the beam has not been detected.

New bunch compressors are being designed using complex simulation programs to calculate the expected emittance dilutions. Unfortunately, the predictions of these codes have never been compared with experimental data. In this Letter, we report on a series of detailed measurements of the beam emittance versus bunch compression using different bunch charges and different energy correlations. We also compare our results with the expectations from a number of simulations and calculations in an attempt to understand the sources of dilution. The two dominant sources appear to be the classical longitudinal space charge force and the coherent radiation.

The experiments were performed using the drive beam at the CLIC Test Facility (CTF-II) at CERN [9]. The CTF-II drive beam line is designed to produce a high charge multibunch beam to test the generation of 30 GHz rf needed for the CLIC two-beam acceleration scheme. It consists of a high-current rf photocathode gun, an S-band accelerating structure that accelerates the beam to $\sim$60 MeV, a magnetic bunch compressor, and four quadrupole triplets, two upstream and two downstream of the compressor, to focus the beam.

The magnetic bunch compressor consists of three C-magnets with rectangular pole shapes. The good field region of the magnets and the size of the vacuum chamber are sufficient to vary the deflection angle of the first magnet between 3.7° and 14.0°, which corresponds to a variation in the energy dependence of the path length $dz/(dE/E) \equiv R_{56}$ from 0.6 to 9 cm.

At this time, five separate scans of emittance versus bunch compression have been performed with different bunch charges and different energy correlations. The measurements were performed by using a single bunch per rf pulse and by using only the portion of the beam line upstream of the CLIC 30 GHz transfer structures.

When performing the measurements, the photocathode laser and the rf gun were optimized to produce the desired charge and then, using the spectrometer, the rf

 0031-9007/00/84(4)/658(4)$15.00

voltage and phase in the S-band accelerating structure were set to produce a 42 MeV beam with the minimum energy spread; this is found by running 5° to 10° forward of the rf crest in the S-band accelerating structure to compensate for the effect of the longitudinal wakefields. At this point, the rf phase was increased by an additional 15° to 25°, depending on the scan, to generate the energy correlation required for bunch compression. The rf voltage was increased to reestablish a 42 MeV beam and then the focusing and steering were optimized to center the beam in the four-beam position monitors and transport the charge without losses.

After the desired beam was established, the bunch compressor magnets were varied to change the degree of compression. Here, the strengths of the first and last bending magnets were set and then the strength of the central magnet was adjusted to recenter the beam in the downstream quadrupole; the strength found in this manner was always very close to the expected value. At periodic intervals, we also checked for residual dispersion by varying the rf phase to change the beam energy; no significant leakage of dispersion was observed.

The beam emittance was determined by measuring the beam spot size while varying one or more of the quadrupoles downstream of the bunch compressor [10]; we should note that, throughout this paper, we will refer to the rms normalized emittance: $\gamma\epsilon_x \equiv \gamma(\langle x^2\rangle\langle x'^2\rangle - \langle xx'\rangle^2)^{1/2}$. The beam spot size was measured using an optical transition radiation (OTR) screen made of polished aluminum with the light from its entrance face imaged on a CCD camera. The horizontal and vertical beam sizes were calculated from the images by taking the rms value of the horizontal and vertical projections of the images after background subtraction. The size calibration is done using three small holes drilled in the screen at a known separation. A range of quadrupole settings were determined to scan through the waist where the spot size was minimized on the OTR screen. The quadrupole strengths were then varied through this range in seven or more steps while the beam size was measured at each step. For each emittance measurement, this cycle was repeated at least twice, and sometimes three times, to determine a statistical error on the spot size measurement.

The bunch length was measured using Cherenkov light from a 0.3 mm sheet of sapphire imaged to a streak camera. The light was filtered by an optical bandpass filter with its transmission maximum in the green. For each bunch compressor setting, ten streak camera measurements were averaged. The resolution of the streak camera is quoted by the manufacturer to be 2 ps FWHM for monochromatic light. However, it is suspected that dispersive effects in the sapphire radiator/optical-path/camera system leads to a resolution limit of about 4 ps which *increases* the optical pulse length.

Two sets of measurements, one with 6 nC per bunch and one with 16 nC per bunch, are summarized in Figs. 1 and 2. For this data, the rf phase was set at about 25° beyond the point of minimum energy spread leading to relatively large energy correlations in the beam. In both cases, the normalized rms horizontal emittance (squares) and the rms bunch length (diamonds) are plotted against the bend angle of the first and last magnets of the bunch compressor. In addition, the measured vertical emittance (circles) is also plotted. However, this measurement is expected to have a large error due to chromatic effects and measurement difficulties, as will be discussed later.

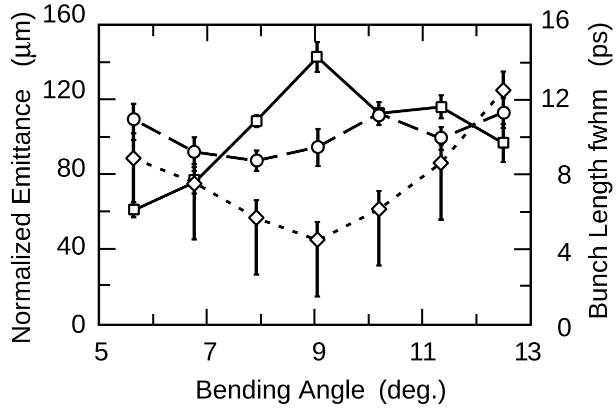

FIG. 1. Measured rms normalized horizontal (squares) and vertical (circles) emittances, and rms bunch length (diamonds) versus angle in the first bend of the compressor with 6 nC.

For many bunch compressor settings, two or more measurements have been made. Each measurement is plotted as an individual point with error bars determined from the statistical measurement error during the scan. The scatter between points is believed to be due to fluctuations in the acceleration rf phase and bunch charge, both of which change the energy correlation in the beam and thereby the degree of bunch compression.

In both of the cases shown in Figs. 1 and 2, the maximum horizontal emittance dilution occurred near the point of maximal compression where the bunch length was the shortest. This behavior was observed in all of our measurements regardless of the bend angle that yielded maximum

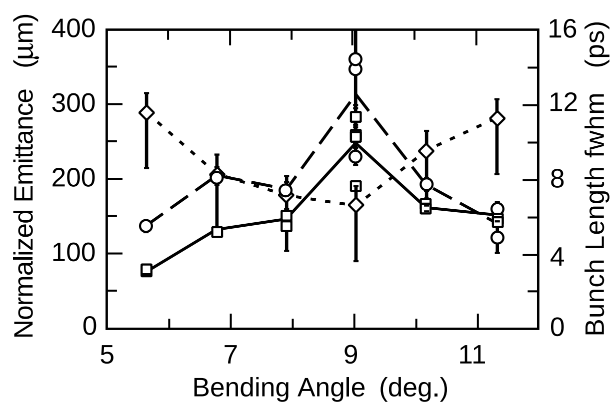

FIG. 2. Measured rms horizontal (squares) and vertical (circles) emittances, and rms bunch length (diamonds) versus angle in the first bend of the compressor with 16 nC.

compression. To illustrate this point, another set of data is plotted in Fig. 3, where the rf phase was set to about 15° beyond the point of minimum energy spread leading to a much smaller energy correlation than in Figs. 1 and 2. This results in the maximum compression and horizontal emittance dilution occurring at a larger R_{56} and therefore a larger bend angle.

To understand these measurements, we have tried to calculate or model all possible sources of emittance dilution. Because the bending magnet strength was the only parameter varied during the scans, the dilution must arise within or possibly downstream of the magnetic chicane. This is also supported by the variation of the beam parameters, i.e., the correlations $\langle x^2 \rangle$, $\langle xx' \rangle$, and $\langle x'^2 \rangle$, which indicates that the dilution originated within the bunch compressor. In studying the dilution sources, we found only the longitudinal space charge and coherent radiation effects to be significant—these increase the horizontal emittance by breaking the achromaticity of the bending magnet system. The sources considered are described below.

First, because of the large energy spread in the beam, which was between 3% and 6% rms depending on configuration, it is possible that the change in edge focusing as the bending magnets were varied, combined with an extreme chromatic sensitivity, may have had some chromatic effect on the emittance or on the emittance measurement procedure. This was studied with 6D particle tracking. In all cases, the chromatic variation in the horizontal plane was calculated to be small.

However, because of the triplet focusing arrangement, the vertical plane was far more sensitive to chromatic errors. In addition, the vertical screen size is much smaller than the horizontal. This makes the measurements difficult since there is a limited dynamic range and the Y measurements are very sensitive to any coupling from the X plane. Because of both the chromatic error and the asymmetry in the vertical measurements, we believe that the vertical emittance measurements are not very reliable and only include the data in the plots for completeness.

Second, we considered the effect of field errors due to the fringing fields or errors in the construction of the bending magnets. The errors required to generate the observed dilution are enormous and the effect would have been clearly visible in the relative field strengths of the bending magnets. Furthermore, field errors cannot account for the shift in the peak of the dilution to larger bending angle when the energy correlation was reduced as illustrated in Fig. 3.

Another possible source of dilution is wakefields due to discontinuities in the CTF vacuum chamber. Actually, the vacuum chamber through the bending magnet region is quite large (2 cm, $\frac{1}{2}$ gap) and will have little effect on the beam and, instead, the most important wakefields come from transitions in and out of the bending magnet chamber to the circular chamber with a 2 cm radius. For the parameters in the CTF-II with 16 nC per bunch, the longitudinal wakefields are calculated to induce an rms energy spread less than 20 keV which is roughly a factor of 50 too small to explain the observations [11,12]. Similarly, assuming a 2 mm transverse offset, the dilution due to the transverse wakefields is 2 orders of magnitude smaller than that measured [13] and can be neglected.

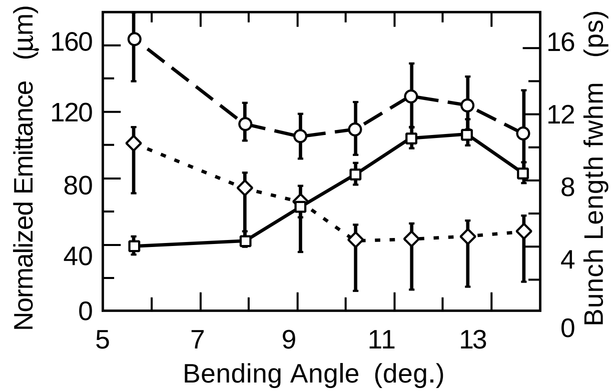

FIG. 3. Measured rms horizontal (squares) and vertical (circles) emittances, and rms bunch length (diamonds) versus current in the first bend of the compressor with 6 nC per bunch and a smaller energy correlation.

Finally, we estimated the dilution due to the classical space charge forces and coherent synchrotron radiation. Assuming 16 nC per bunch with a fully compressed rms bunch length of 200 μm and a 9° bending angle, analytic estimates for the emittance dilution due to the transverse space charge force [1] yield $\Delta\gamma\epsilon_x \approx 4$ mm mrad while the transverse field of the coherent radiation [14] is estimated to cause an emittance dilution of $\Delta\gamma\epsilon_x \approx 6$ mm mrad; both of these dilutions are much smaller than that observed. In contrast, the longitudinal space charge force is estimated [1] to cause a dilution, which adds in quadrature to the initial emittance, of $\Delta\gamma\epsilon_x \approx 50$ mm mrad while the rms energy spread induced by the coherent radiation is expected [5] to be about 2% which, from 6D tracking calculations, causes $\Delta\gamma\epsilon_x \approx 100$ mm mrad; note that shielding of the radiation by the vacuum chamber is expected to be important only for bunch lengths greater than [2] $\sigma_z \gtrsim \sqrt{h^2 w/\pi^2 \rho}$, where h and w are the vacuum chamber height and width and ρ is the bending radius. In the CTF-II, this corresponds to a bunch length of 3 mm and, with sub-mm compressed bunch lengths the shielding should have little effect.

To further study these sources, we used the computer code PARMELA to simulate the space charge forces and a 6D tracking simulation, referred to as CSR-TRACK, that includes an approximate representation for the coherent radiation force based on the results of Ref. [6]. To compare with the results of Ref. [6], we note that in all cases the CTF-II operated in the "long-magnet, short-bunch" regime as would most high-energy bunch compressors. In the simulations, the initial beam emittances and beam parameters were fitted to agree with those measured at the smallest bend angles, and the bunch length and rf phases were chosen to provide the best fit to the bunch length measurements. In all cases, minimal variation of

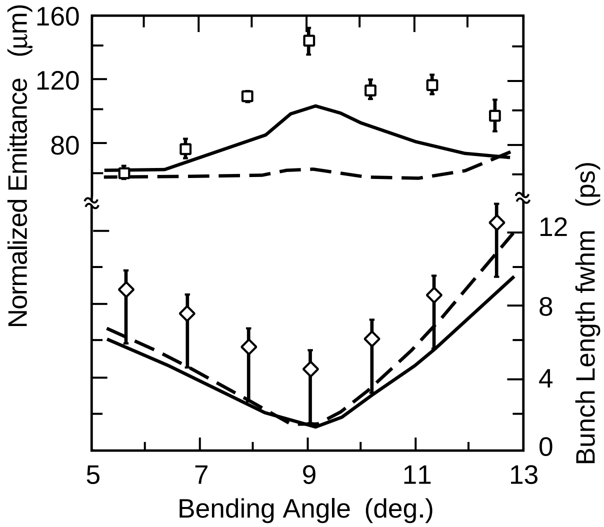

FIG. 4. Comparison of the measured rms horizontal emittance (squares) and rms bunch length (diamonds) with PARMELA (dashed lines) and CSR-TRACK (solid lines) for 6 nC per bunch.

the vertical emittance was observed; however, substantial horizontal dilution was calculated which, although smaller in magnitude, agrees qualitatively with the measurements in that the maximum dilution occurs close to the point of maximal compression. Similarly, the variation of the second moments in simulation, i.e., $\langle x^2 \rangle$, $\langle xx' \rangle$, and $\langle x'^2 \rangle$, agree qualitatively with those measured which, as mentioned earlier, implicate an emittance source in the chicane. The simulated horizontal emittance and bunch length are compared in Fig. 4 with the data from Fig. 1, while the higher charge data, plotted in Fig. 2, is compared with the simulated emittance in Fig. 5.

In conclusion, we have observed large emittance growth during bunch compression at the CTF-II. This growth is maximum close to the point of maximal compression and decreases when the bunch is undercompressed or overcompressed. Because no upstream components were varied during the measurements and because of the observed variation in the beam parameters, the emittance dilution would appear to originate in the magnetic chicane. However, because the dilution does not depend on the absolute strength of the bending magnets in the chicane but instead depends on the degree of compression which can be varied by changing the incoming energy correlation, the dilution is not consistent with field errors in the bending magnets; this is also supported by linear tracking of the bend magnet strengths and by the absence of any dispersion observed leaking from the chicane. Finally, the emittance dilution appears to increase with bunch charge but cannot be explained by wakefields due to the vacuum chamber through the CTF.

Based on simulation and analytic calculations, only two sources could generate the observed dilutions: the classical longitudinal space charge force and coherent synchrotron radiation. Simulations of both effects yield dependences on the bunch compressor settings similar to those observed. However, in the simulations, the emittance dilution due to the longitudinal space charge force was less than 10% of that observed, while that due to the coherent radiation was roughly 50% of that observed. After upgrades to the CTF accelerator structures, measurements should be possible at higher beam energy which will allow a clearer separation of the dilution sources.

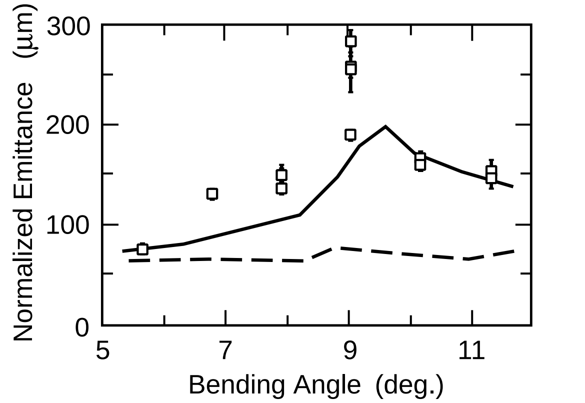

FIG. 5. Comparison of the measured rms horizontal emittance (squares) with PARMELA (dashed line) and CSR-TRACK (solid line) for 16 nC per bunch.

*Present address: Stanford Linear Accelerator Center, Stanford, California.

[1] B. E. Carlsten and T. O. Raubenheimer, Phys. Rev. E **51**, 1453 (1995).
[2] R. Warnock and P. Morton, Part. Accel. **25**, 113 (1990).
[3] K. Ng, Part. Accel. **25**, 153 (1990).
[4] J. Murphy *et al.*, Part. Accel. **57**, 9 (1997).
[5] Y. Derbenev *et al.*, (DESY) Report No. TESLA-FEL 95-05, 1995 (unpublished).
[6] E. Saldin, E. Schneidmiller, and M. Yurkov, (DESY) Report No. TELSA-FEL 96-14, 1996 (unpublished).
[7] T. Nakazato *et al.*, Phys. Rev. Lett. **63**, 1245 (1989).
[8] E. Blum, U. Happek, and A. Sievers, Nucl. Instrum. Methods Phys. Res., Sect. A **307**, 568 (1991).
[9] H. Braun *et al.*, in *Proceedings of the Fifth European Conference on Particle Accelerators, Spain, 1996* (Institute of Physics, Philadelphia, 1996), p. 42.
[10] P. Tenebaum *et al.*, in *Proceedings of the 1997 Particle Accelerator Conference, Vancouver* (IEEE, Piscataway, NJ, 1997).
[11] L. Palumbo, Part. Acc. **25**, 201 (1990).
[12] F. Zimmermann and A. Chao, in *Proceedings of the Fifth European Conference on Particle Accelerators, Spain, 1996* (Institute of Physics, Philadelphia, 1996).
[13] E. Gianfelice and L. Palumbo, IEEE Trans. Nucl. Sci. **37**, 1084 (1990).
[14] Y. Derbenev and V. Shiltsev, Report No. SLAC-PUB-7181, 1996 (unpublished).